

Original Article

Screening and analysis of differentially expressed genes of human melanocytes in skin cells mixed culture

Xingyu Mei, Zhouwei Wu, Jie Huang, Yue Sun, Weimin Shi

Department of Dermatology, Shanghai General Hospital, Shanghai Jiao Tong University School of Medicine, Shanghai 200080, China

Received January 1, 2019; Accepted April 10, 2019; Epub May 15, 2019; Published May 30, 2019

Abstract: Background: This study aims to screen the key genes and possible signaling pathways involved in the differentiation and proliferation of human melanocytes (MCs) by in vitro culture of mixed skin cells. This will be helpful to further study the mechanisms and treatment strategies of pigment-related diseases such as vitiligo. Methods: Mixed skin cells were obtained by digesting and separating normal human foreskin tissues. Ribonucleic acid (RNA) was extracted from sorting cells and high-throughput transcriptome sequencing was performed at different culture time points. Differentially expressed genes (DEGs) were obtained by comparing the expression abundance of genes at different culture time points. Then the key genes and signaling pathways involved in the differentiation and proliferation of MCs were screened and verified by real-time quantitative polymerase chain reaction (qPCR) test. Results: Twenty one DEGs were finally screened for further qPCR validation, mainly involved in 4 signaling pathways. The expressions of Wnt5A, Wnt5B, FZD2 and FZD3 in Wnt pathway were continuously up-regulated, and that of Wnt4 gene was continuously down-regulated, however, all the above hadn't been verified by qPCR. The expressions of COL5A2, COL6A3, ITGB1, ITGA4, ITGAV, AKT3, PIK3CD, PIK3R1 and PIK3R2 in phosphoinositide 3-kinase (PI3K) pathway were continuously up-regulated, of which PIK3CD, PIK3R2, COL5A2, ITGA4, ITGAV and AKT3 were verified by qPCR. PDGFB and GRB2 gene expressions were down-regulated in platelet-derived growth factor (PDGF) pathway, while PDGFRB was continuously up-regulated, of which PDGFB and PDGFRB were verified. The DHRS3, DHRS9, RDH10 and SDR16C5 genes in retinol metabolic pathway were continuously down-regulated and verified by qPCR. Conclusion: We suggested that Wnt5A gene in Wnt/ β -catenin classical pathway, integrin combining with extracellular matrix through PI3K signaling pathway, retinoic acid catabolism-related genes could promote the differentiation and proliferation of MCs; however, PDGFB gene might have a negative regulatory effect on the growth of MCs.

Keywords: Melanocytes, pigment-related disease, transcriptome sequencing, differentially expressed genes, signaling pathway

Introduction

Vitiligo is an acquired depigmentation disorder with a worldwide incidence ranging from 0.1% to 8% [1]. Traditional treatments such as medication and phototherapy have some curative effects; however, the success rate is less than 50% [2]. Given this, surgical treatment techniques such as epidermal transplantation, microporous transplantation and melanocytes (MCs) transplantation have recently emerged [3], with autologous epidermal transplantation being the most widely used method in clinical practice. The key feature of this method is that MCs and other mixed skin cells are cultured in vitro to obtain an expanded area of epidermal membrane and then transplanted.

MCs produce and maintain pigments in humans and other vertebrates [4]. Melanosomes in MCs synthesize and deliver melanin particles to adjacent keratinocytes (KCs) to produce the color in skin and hair. In addition to maintaining the color of skin and hair, MCs also block damage from ultraviolet radiation [5]. KCs regulate the morphology, melanin synthesis and transport of MCs by secreting growth factors or extracellular matrix components [6]. Melanocyte stem cells (MSCs) are slow-cycle primitive cells that cannot synthesize melanin particles but act as MCs repositories [7]. In 2002, Lu et al. [8] screened compounds that interfere with melanogenesis using a co-culture model established with mixed cells and found different results from those obtained by using MCs

Screening and analysis of human melanocytes genes

alone. Therefore, direct co-culture of MCs, KCs and MSCs can better simulate the process of melanogenesis in vitro and provide the opportunity to study the mechanism of proliferation and differentiation of MCs, which is important for the discovery of therapeutic strategies for pigmentation diseases.

The transcriptome is the total RNA transcribed from specific tissues or cells at a certain growth stage. The rapid development of molecular biology technology in recent decades has made it possible to study transcriptomes and their function. High-throughput RNA sequencing (RNA-seq) is based on the principle of reverse transcription of RNA into complementary deoxyribonucleic acid (cDNA) and sequencing of cDNA. The results of RNA-seq are directly compared with the reference gene, and the genes of interest are obtained by differential analysis of gene expression. RNA-seq has the advantages of high throughput, low cost, high sensitivity and good repeatability [9].

At present, our understanding of the mechanism of proliferation, differentiation and melanogenesis of MCs is mainly based on mouse MCs [10]. The MCs of mice are mainly located in the hair bulb region of dermal hair follicle, whereas human MCs are mainly located in the epidermal basement membrane. In addition, previous studies investigating MCs often use a separate culture method and neglect the regulation function of other skin cells, which does not completely simulate the physiological status of MCs in vitro [8]. In this study, high-throughput RNA-seq of MSCs and mature MCs obtained from human skin mixed cell culture was performed to screen key genes related to the differentiation and proliferation of human MCs. The analysis of related signaling pathways will provide a novel approach to study the mechanism of MCs differentiation and proliferation and help to further characterize the pathogenesis and treatment strategies of pigment-related diseases.

Materials and methods

Skin tissue

Normal prepuce tissue was collected from 20 to 50-year-old males circumcised in the Urology Department of Shanghai General Hospital from February 2017 to December 2017. All patients provided informed consent to having their tissue used in the experiment.

Magnetic separation of PAX3+ cells and Melan-A+ cells in mixed skin cells

Magnetic beads labeled with biotin, PAX3 antibody and Melan-A antibody were incubated overnight at 4°C. The previously digested mixed skin cells were taken out from the incubator and centrifuged to discard the supernatant. The PAX3 and Melan-A antibodies with magnetic beads were added to label MSCs and mature MCs, respectively and incubated at room temperature for 90 min. The cells were placed in MS separation column to collect the cells labeled with corresponding magnetic beads.

RNA extraction and detection of sorting cells

Trizol was added to the cell sample and the supernatant was added to a new centrifuge tube. Chloroform was added and incubation was carried out for 15 min at room temperature until the sample was stratified. The upper aqueous phase of the sample was added to a new centrifugal tube, incubated at -80°C for 30 min after glycogen and isopropanol were added. The supernatant was removed after centrifugation and the RNA precipitation was washed using 75% ethanol and the RNA precipitation was air-dried for 5 min. The purity and concentration of 500 ng RNA was detected by nanodrop after electrophoresis and the integrity of RNA was detected using Agilent 2100. If A260/A280 ranged from 1.8 to 2.1 and RNA integrity number was larger than 7, the total RNA was used for subsequent experiments.

Establishment of sequencing library and sequencing of transcriptome

Cellular mRNA was enriched by magnetic beads with Oligo (dT) and randomly interrupted by the addition of fragmentation buffer. The cDNA chain was synthesized using mRNA as a template and cDNA library was enriched by PCR and constructed with Qubi (Invitrogen) for qPCR verification. Sequencing with Illumina HiSeq 2500 yielded a large amount of high-quality raw data from P0, P1, P2 and P3 cell samples. High-quality clean reads were obtained by filtering out the junctions and low-quality bases.

Gene expression and DEGs screening

The reads obtained from each sample were compared with the human reference gene sequence library (hg19, GRCh37 Genome Reference Consortium Human Reference 37) to

Screening and analysis of human melanocytes genes

obtain mapped reads. According to the comparison results, expression level was estimated and the abundance of corresponding single gene sequence was indicated as fragments per kilo base of Transcript per million mapped reads (FPKM). Differential expression analysis was performed by EBSseq, and the significant *P*-value obtained from original hypothesis test was corrected using the Benjamini-Hochberg method. Finally, the corrected *P*-value, namely false discovery rate, was used as the key indicator of screening DEGs. *P*-values < 0.05 were considered statistically significant.

Western blot

The Western blot analysis was conducted as previously described [8]. MCs were washed with saline and harvested by scraping the culture dishes followed by pyrolysis buffer. The buffer was cooling for 40 minutes using an ice bath and centrifuged for 20 minutes. After discarding the supernate, the protein concentration was assessed using the BCA protein assay. Proteins were then transferred to polyvinylidene difluoride (PVDF) membranes and blocked by 5% nonfat milk for 2 h at 37°C. After rinsing, the membranes were incubated at 4°C overnight with primary antibodies. After being washed with Tris buffer solution, the secondary antibody was added to the solution and incubated for 1 h. Binding was detected by western lightning plus ECL reagent (Waltham, MA, USA). Densitometric analysis was quantified with Image-J software.

Functional annotation and enrichment analysis of DEGs

To further analyze the gene products involved in signaling pathways and their biological functions, DEGs were compared with Kyrto Encyclopedia of Genes and Genomes (KEGG) and Gene Ontologo (GO) databases by DAVID (<http://david.abcc.ncifcrf.gov/>).

qPCR verification of DEGs

The relative expression of selected DEGs in each sample was detected by q-PCR. The previously qualified total RNA was reversely transcribed into cDNA and the reverse transcription reaction system is shown in [Table S1](#). Real-time PCR amplification system and verification genes are shown in [Table S2](#). Three independent experiments were performed for each sample. The Ct values were calculated after the opera-

tion of fluorescence detection and plotting the melting curve.

Statistical analysis

All statistical analyses were performed using SPSS 19.0. Real-time PCR data was presented as means ± standard error. One way-ANOVA with a Turkey's post-hoc test was used for comparison of multiple groups and Student's t-test was used for comparison between two groups. *P* values of 0.05 or less were considered statistically significant.

Results

Sorting of PAX3+ cells and Melan-A+ cells in mixed skin cells

The skin cells of normal human prepuce tissue were mixed and cultured in vitro and subcultured every 10 days when growth density reached about 85%. The ratios of PAX3+ and Melan-A+ cells in primary and each passage generation (P0, P1, P2, and P3) mixed cell samples ranged from 7.6% to 9.3%, which decreased gradually with the time of culture ([Table S3](#)).

RNA extraction and detection of sorting cells

The A260/A280 values of RNA in each sample ranged from 1.9 to 2.0 in quality control detection. The total sample was enough for more than two experiments ([Table S4](#)), and there wasn't any degradation and pollution phenomenon after electrophoresis. RIN values detected by Agilent 2100 Bioanalyzer were greater than 8 (**Figure 1**), indicating that the quality requirements were met for subsequent experiments.

Data output statistics of transcriptome sequencing

The output statistics for each RNA sample are shown in [Table S5](#). The clean reads were compared with the reference genome sequence and the ratios of bases in each sample with a quality above Q30 were greater than 85%. The alignment efficiency (mapped reads/clean reads × 100%) of P0, P1, P2, and P3 samples was 87.1%, 86.6%, 87.1%, and 83.5%, respectively. Results found that 40~60% of the aligned clean reads were distributed in the coding area, followed by 30% in the untranslated area; followed by 5~15% and 6~14% distribu-

Screening and analysis of human melanocytes genes

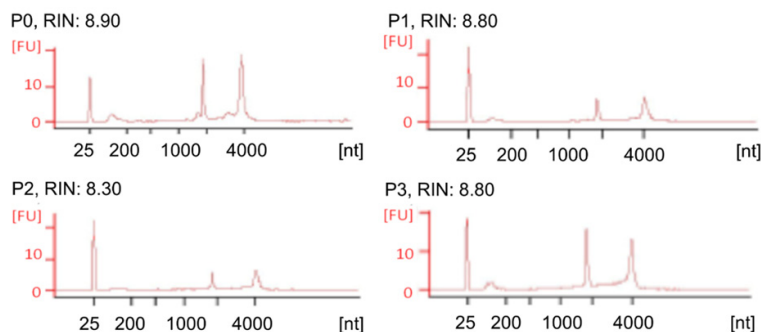


Figure 1. Total RNA electrophoresis and tests of different generations (P0, P1, P2, and P3) through Agilent 2100 Bioanalyzer. All the RIN values were greater than 8.

tion in intron and intergenic regions respectively (**Figure 2A**). The total numbers of sequenced genes in each sample compared with the reference genome are shown in [Table S6](#). The number of encoding protein genes in P0, P1, P2 and P3 samples was 25331, 23017, 23236 and 22331, respectively.

Statistics of DEGs

The FPKM of aligned genes in P1, P2, and P3 samples were compared with P0 sample and the number of DEGs were counted ($P < 0.05$) ([Table S7](#)). The numbers of DEGs in P1, P2 and P3 samples increased with the prolongation of culture time. The number of down-regulated DEGs was significantly more than up-regulated DEGs. The top 20 up-regulated and down-regulated DEGs in each comparison group are shown in [Tables S8, S9, S10](#). The number of common DEGs in each comparison group are shown in **Figure 2B**.

GO analysis of DEGs

To further understand the function of DEGs, GO enrichment analysis was performed. The DEGs were enriched to 189, 166 and 222 functional annotations respectively in three categories: cellular component, molecular function and biological process ([Table S11](#)). Functional annotations were most abundant in the biological process category, of which signal transduction was enriched with the most genes. The DEGs were specifically grouped into different functional annotations under each category (**Figure 3**).

KEGG pathway functional annotations of DEGs

To analyze genes that were significantly enriched into signaling pathways, DEGs were analyzed by DAVID for KEGG pathway enrichment. The DEGs of P1 vs P0 group were enriched into 31 signaling pathways, whereas DEGs of P2 vs P0 and P3 vs P0 group were enriched into 17 and 19 signaling pathways, respectively. The top 10 signaling pathways with the most DEGs involved

in each comparison group are shown in [Table S12](#).

Analysis of DEGs with continuously up or down regulated expression

The number of DEGs with continuously up-regulated expression level in three comparison groups was 2733, and 1589 for DEGs with continuously down-regulated expression level. The DEGs that were continuously up or down regulated were analyzed by DAVID for KEGG pathway enrichment. The genes with continuously up-regulated expression were enriched into 47 pathways, and 18 pathways for the genes with continuously down-regulated expression. The top 10 signaling pathways with the most DEGs are shown in [Table S13](#). Metabolic pathways enriched by continuously up-regulated genes contained the largest number of genes, followed by PI3K-AKT signaling pathway. MAPK signaling pathway which was enriched by continuously down-regulated genes contained the largest number of genes. These DEGs were analyzed by DAVID for GO enrichment (**Figures 4, S1**). Most were enriched into the cellular component category with the biological processes having the lowest number of DEGs.

qPCR verification of DEGs

Based on the previous GO and KEGG enrichment analysis of DEGs in each sample, 21 DEGs were screened for further qPCR verification. This involved 4 signaling pathways. The first was the Wnt pathway: Wnt4, Wnt5A and Wnt5B genes hadn't been further verified in real-time PCR due to the failure to achieve

Screening and analysis of human melanocytes genes

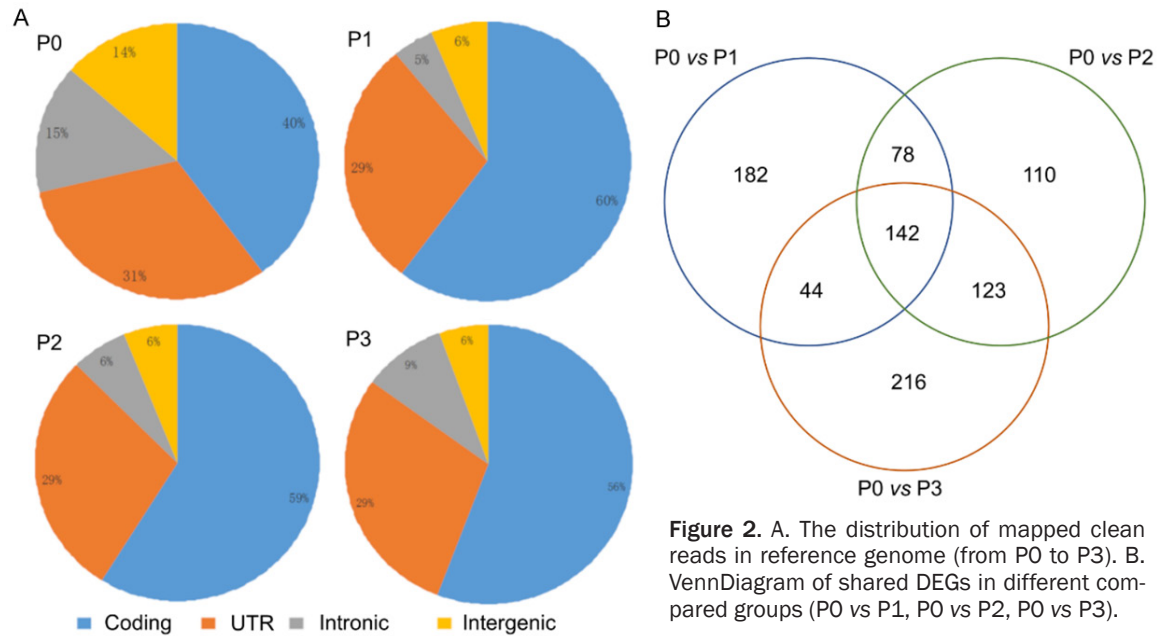


Figure 2. A. The distribution of mapped clean reads in reference genome (from P0 to P3). B. VennDiagram of shared DEGs in different compared groups (P0 vs P1, P0 vs P2, P0 vs P3).

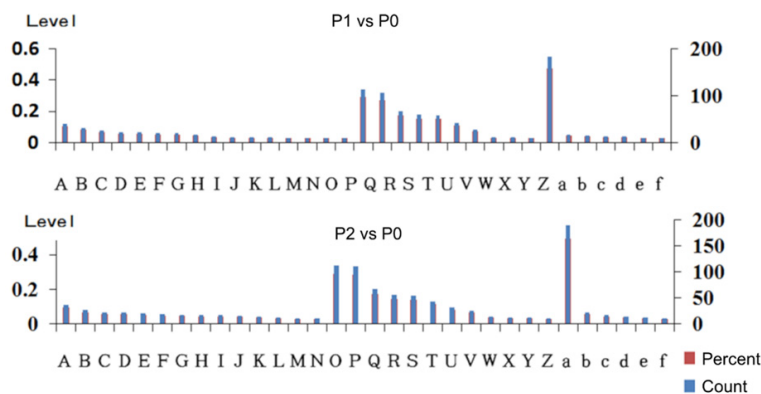


Figure 3. GO analysis of DEGs in different groups. A. Signal transduction. B. Positive regulation of transcription from RNA polymerase II promoter. C. Immune response. D. Apoptotic process. E. Cell adhesion. F. Inflammatory response. G. Positive regulation of GTPase activity. H. Positive regulation of ERK1 and ERK2 cascade. I. Cell-cell signaling. J. Cellular response to tumor necrosis factor. K. Chemotaxis. L. Angiogenesis. M. Chemokine-mediated signaling pathway. N. Response to lipopolysaccharide. O. Regulation of immune response. P. MAPK cascade. Q. Cytoplasm. R. Plasma membrane. S. Extracellular region. T. Extracellular space. U. Integral component of plasma membrane. V. Cell surface. W. Apical plasma membrane. X. Cytoskeleton. Y. External side of plasma membrane. Z. Protein binding. a. Receptor binding. b. Receptor activity. c. Structural molecule activity. d. Protein kinase activity. e. Cytokine activity. f. Transcriptional activator activity. Most of these DEGs were enriched into cellular component category.

amplification; the expression level of FZD2 and FZD3 significantly decreased with the prolongation of culture time in real-time PCR experiment ($P < 0.05$). These results were different from the result in RNA-seq (Figure 5). The second was the PI3K-AKT pathway: COL5A2, COL6A3,

ITGB1, ITGA4, ITGAV, PIK3R1, PIK3R2, PIK3CD and AKT3 genes were gradually increased in RNA-seq with prolonged culture time (Figure 6) and a similar indication was presented through the protein expressions of some relevant genes (Figures 7, S2, S3, S4 and S5). In real-time PCR verification, the results of PIK3CD and PIK3R2 were consistent with the previous; the results of COL5A2, ITGA4, ITGAV and AKT3 were approximately identical; COL6A3, ITGB1 and PIK3R1 genes didn't achieve consistent results (Figure 6). The third was the PDGF pathway: the expression of PDGFB in real-time PCR gradually decreased in P1, P2 and P3 samples ($P < 0.05$), which was consistent with the result in RNA-seq, and a similar indication was presented through the protein expressions of some relevant genes (Figures 8, S6, S7, S8 and S9). PDGFRB expression was increased with the prolongation of culture time, which was consistent with the RAN-seq; while the expression of GRB2 gene was the opposite (Figure 9). The fourth was the retinol metabolism pathway:

Screening and analysis of human melanocytes genes

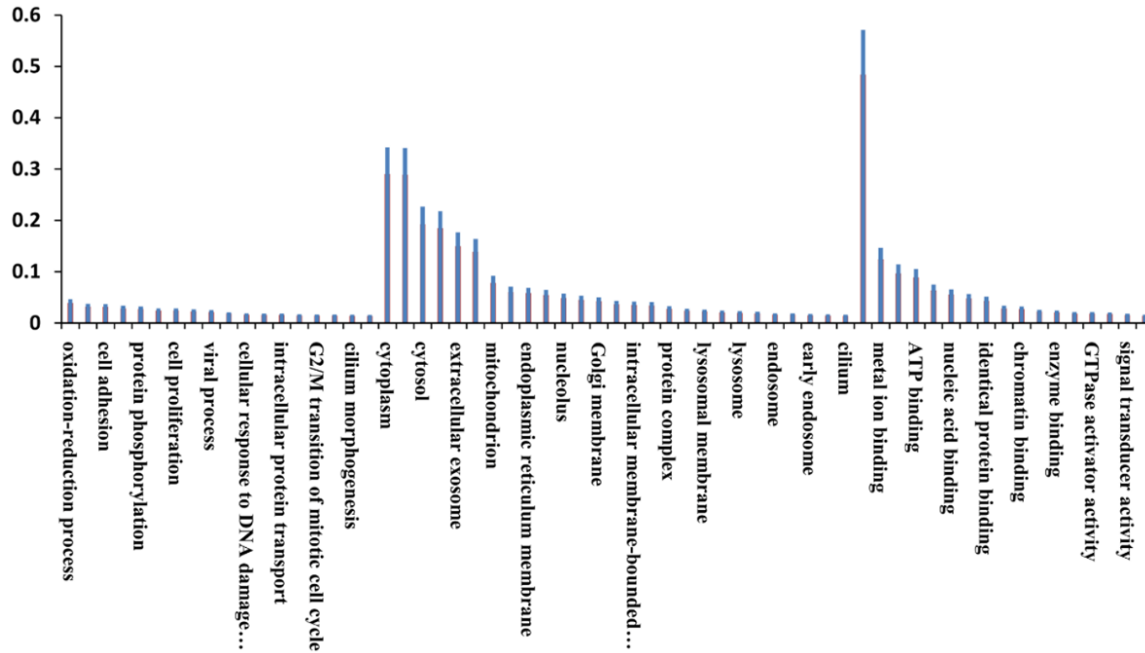


Figure 4. GO analysis of DEGs with continuously increased expression.

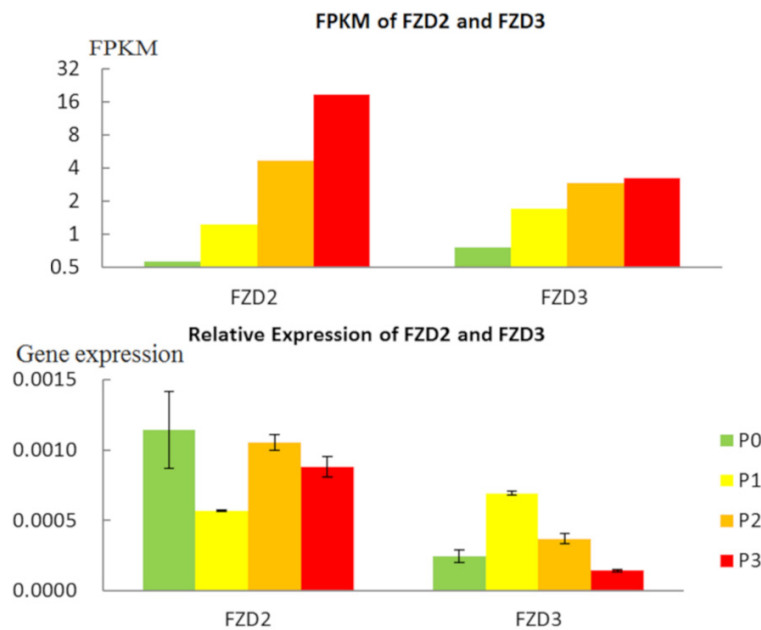


Figure 5. FPKM and relative expression of FZD2 and FZD3 in RNA-seq and real-time PCR. The expression level of FZD2 and FZD3 significantly decreased with the prolongation of culture time in real-time PCR experiment, which was different from the result in RNA-seq.

the expression levels of DHRS3, DHRS9, RDH10 and SDR16C5 genes in RNA-seq were consistent with the results in real-time PCR, which gradually decreased in P1, P2 and P3 samples ($P < 0.05$) (**Figure 10**).

Discussion

At present, several studies have performed high-throughput transcriptome sequencing on human MCs. In 2014, Haltaufderhyde et al. [11] used SOLiD sequencing technology to perform whole gene transcriptome sequencing of human skin tissue consisting of MCs, KCs and MSCs to compare the gene expression differences between MCs and other cells. In 2016, Sun et al. [12] used Illumina sequencing platform to perform transcriptome sequencing of KCs and MCs isolated from human prepuce tissue before and after ultraviolet irradiation. In this study, Illumina HiSeq 2500 platform was used to conduct high-throughput transcriptome sequencing of MCs and MSCs cultured in vitro.

In our study, the ratio of bases in each sample with a quality rating above Q30 was greater than 85% indicating the high precision of this sequencing. The total reads of each sample was greater than 4×10^7 and the alignment

Screening and analysis of human melanocytes genes

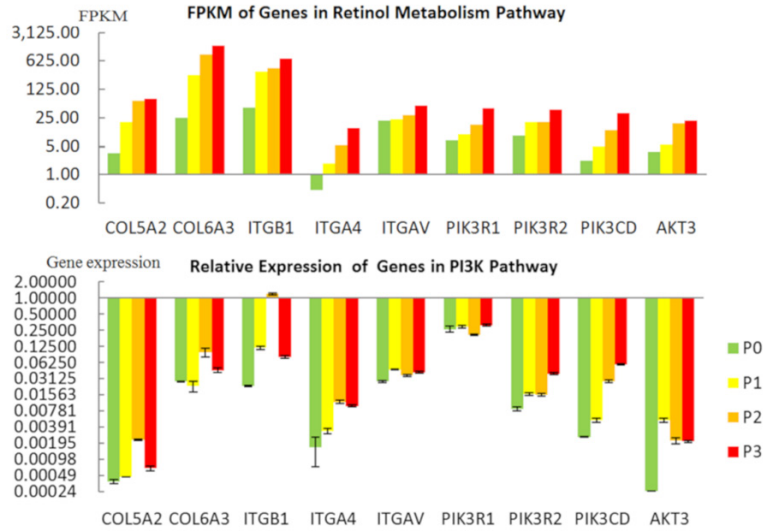


Figure 6. FPKM and relative expression of PI3K-AKT pathway related genes in RNA-seq and real-time PCR. The results of PIK3CD and PIK3R2 were consistent with the RNA-seq; the results of COL5A2, ITGA4, ITGAV and AKT3 were approximately identical; COL6A3, ITGB1 and PIK3R1 genes didn't achieve consistent results.

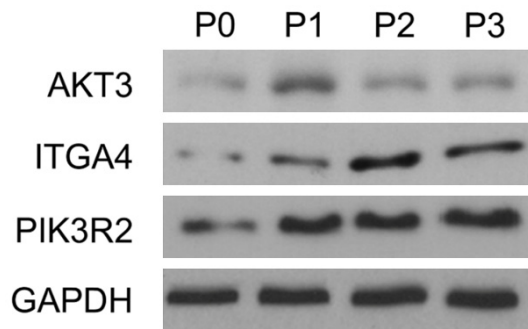


Figure 7. Protein expressions of several genes (AKT3, ITGA4, PIK3R2) in PI3K pathway in different generations.

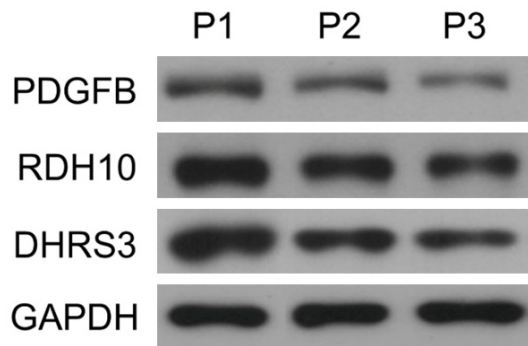


Figure 8. Protein expressions of several genes (PDGFB, RDH10, DHRS3) in PDGF pathway in different generations.

efficiency with human reference gene sequence library was as high as 83~88%. Most of the clean reads were located in the coding region, indicating that the sequencing results were not impacted by immature mRNA and genome annotation was adequate. The number of down-regulated genes was significantly more than that of up-regulated genes in each comparison group, indicating that some genes were down-regulated or not expressed with the differentiation and maturation of MCs.

In GO enrichment analysis of DEGs, functional annotations were most abundant in the biological process category, which was consistent with the differentiation and proliferation process of MCs cultured in vitro. The annotation with the most genes was signal transduction in the biological process category, indicating that signal transduction played an important role in differentiation and proliferation of MCs. In the cellular component category, DEGs were mainly concentrated in the plasma membrane an integral component of the membrane. In the molecular function category, DEGs were mainly concentrated in protein binding functions, indicating that cell membrane protein components and protein binding functions significantly changed with the differentiation and maturation of MCs. In KEGG pathway enrichment analysis of DEGs, we discovered that the cytokin-cytokine receptor interaction pathway contained the most enriched genes, indicating that DEGs played an important regulatory role in the differentiation and proliferation of MCs. Subsequently, the number of genes with continuously up-regulated FPKM was greater than down-regulated genes in P0, P1, P2, and P3 samples, indicating the continuous dividing ability and high proliferative activity of MCs.

Wnt is a type of secreted glycoprotein, which can be divided into Wnt1 and Wnt5A. Wnt signaling pathway is involved in cell migration, pro-

Screening and analysis of human melanocytes genes

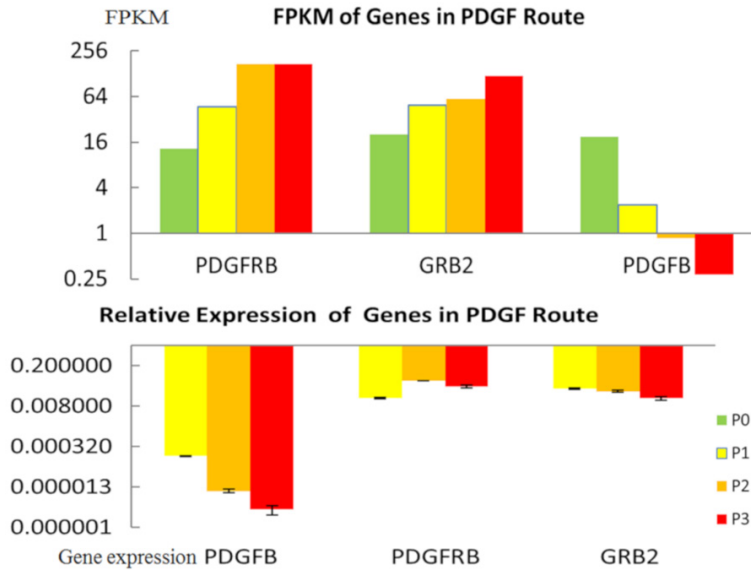


Figure 9. FPKM and relative expression of PDGF route related genes in RNA-seq and real-time PCR. The expression of PDGFB in real-time PCR was gradually decreased in P1, P2 and P3 samples, which was basically consistent with the result in RNA-seq; PDGFRB expression was increased with the prolongation of culture time, which was consistent with the RNA-seq; while the expression of GRB2 gene was opposite to the previous result.

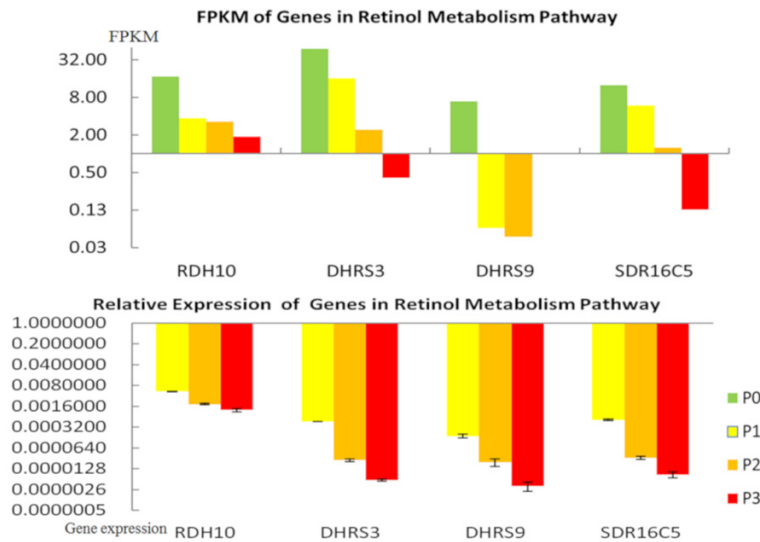


Figure 10. FPKM and relative expression of retinol metabolism route related genes in RNA-seq and real-time PCR. The expression levels of DHRS3, DHRS9, RDH10 and SDR16C5 genes in RNA-seq were consistent with the results in real-time PCR, which decreased gradually in P1, P2 and P3 samples.

liferation, differentiation, and self-renewal of stem cells [13]. Wnt signaling pathway includes the classic Wnt/ β -catenin and non-classic Wnt pathway. Wnt1 protein is involved in the signal transduction of the classic pathway; while

Wnt5A protein is involved in the non-classic pathway [14]. A large number of studies have revealed that the classic Wnt/ β -catenin signaling pathway plays a crucial role in the development of MCs [15]. It is generally considered that Wnt5A acts primarily through the non-classic Wnt pathway and inhibits the classic Wnt/ β -catenin pathway to regulate the differentiation of MCs [14]. In this sequencing, we discovered that the expression levels of genes related to the Wnt pathway continuously changed with the culture of MCs in vitro, suggesting that the Wnt5A gene might promote the differentiation and maturation of MCs through Wnt/ β -catenin classic pathway.

Currently, several studies [16, 17] report that Wnt4 can be used as a gene marker for melanoma. In this sequencing, the Wnt4 gene expression with culture time was low, indicating that the cultured MCs don't have a tendency to evolve into tumor cells. However, Wnt4, Wnt5A, and Wnt5B genes were not further validated in real-time PCR for some technical reasons; FZD2 and FZD3 didn't achieve consistent results with high-throughput transcriptome sequencing. We will validate gene expressions of this pathway in a future sample-expanded study.

PI3K family is a kind of kinase that specifically catalyzes phosphatidylinositol lipids. PI3K can respond to various intracellular and extracellular information through hormone receptors, transmembrane tyrosine kinase receptors and cytokines and then regulate cell growth, proliferation, differentiation and apoptosis [18].

Screening and analysis of human melanocytes genes

Some scholars believed that the PI3K/AKT signaling pathway plays an important role in the pathogenesis of melanoma and promotes the transformation of MCs [19, 20]. In real-time PCR validation, the results of ITGA4, ITGAV, AKT3, PIK3CD, and PIK3R2 genes were consistent with high-throughput transcriptome sequencing. Therefore, we hypothesized that after combining with integrin, extracellular matrix activated the downstream factors related to cell proliferation and cycle through the PI3K-AKT signaling pathway and as a result, regulated the proliferation and survival of MCs.

PDGF belongs to the tyrosine protein kinase family, which regulates a variety of cellular functions, such as proliferation, differentiation, and activation of signal transduction by binding to specific receptors [21]. PDGF has two genes, PDGFA and PDGFB. In this RNA-seq, the number of PDGFB gene copies gradually decreased with the prolongation of culture time and was verified by real-time PCR. Therefore, PDGFB may have a negative regulatory effect on the proliferation of MCs in vitro, which was consistent with Pazos et al. [22]. However, the number of its receptor gene copies, PDGFRB, gradually increased with the prolongation of culture time and was verified by real-time PCR. Some studies [23, 24] have shown that PDGFR might also play a role in the occurrence of melanoma and the differentiation and maturation of MCs, however, the exact effect of PDGFR requires further study.

Vitamin A is a fat-soluble vitamin that can be converted into bioactive substances such as retinol, retinaldehyde and retinoic acid through a series of biological processes in vivo [25]. Retinol can be oxidized to retinaldehyde under the action of retinol dehydrogenase 10 (RDH10). RDH10 belongs to the 16c family of short chain dehydrogenase/reductase (SDR) superfamily proteins [26]. Dehydrogenase/reductase 3 (DHRS3) and DHRS9 both belong to SDR superfamily proteins that can convert retinaldehyde to retinol. In vivo, retinaldehyde is oxidized to retinoic acid by retinal dehydrogenase, and the most important enzyme involved in retinoic acid catabolism is CYP26, a member of cytochrome P450 family [27]. In this real-time PCR experiment, the previous results of RDH10, SDR16C, 5DHRS3, DHRS9 and CYP26B1 genes were confirmed. Therefore, the differentiation and proliferation of MCs may be

accompanied by an increase in the expression of genes involved in retinoic acid catabolism and a decreased in the expression of synthesis-related genes. As a result, the catabolism of retinoic acid may contribute to the differentiation, proliferation and maturation of cultured MCs. However, the exact mechanism and the impact to proliferation and differentiation of MCs requires further study.

Compared with previous whole-genome transcriptome sequencing of human MCs, in this study MCs were mixed with other skin cells to mimic the microenvironment of MCs in vivo so the differentiation and proliferation was closer to typical physiological conditions. Second, magnetic beads were used to obtain undifferentiated MSCs and mature MCs for RNA-seq, whereas previous studies have only been based on mature MCs. Third, the whole genome RNA-seq was performed at different time points, which was helpful for the discovery and screening of key DEGs and related signaling pathways. Several limitations exist in this study. First, several key genes of related signaling pathways were not verified by real-time PCR due to some technical reasons. Second, the results of some DEGs in real-time PCR didn't achieve consistent results with high-throughput transcriptome sequencing. All of the above and the exact mechanisms of key genes requires further study.

Conclusion

In conclusion, results suggest that the Wnt5A gene in the Wnt/ β -catenin classic pathway, integrin combining with extracellular matrix through PI3K-AKT signaling pathway, and retinoic acid catabolism-related genes could promote the differentiation and proliferation of MCs and the PDGFB gene may have a negative regulatory effect on the growth of MCs.

Acknowledgements

This work was supported by the National Natural Science Foundation of China (Grant No. 81703140 and No. 81703140).

Disclosure of conflict of interest

None.

Screening and analysis of human melanocytes genes

Address correspondence to: Weimin Shi, Department of Dermatology, Shanghai General Hospital, Shanghai Jiao Tong University School of Medicine, Shanghai 20008, China. E-mail: docshiwm@163.com

References

- [1] Hua C, Boussemaert L, Mateus C, Routier E, Boutros C, Cazenave H, Viollet R, Thomas M, Roy S, Benannoune N, Tomasic G, Soria JC, Champiat S, Texier M, Lanoy E and Robert C. Association of vitiligo with tumor response in patients with metastatic melanoma treated with pembrolizumab. *JAMA Dermatol* 2016; 152: 45-51.
- [2] King YA, Tsai TY, Tsai HH and Huang YC. The efficacy of ablation-based combination therapy for vitiligo: a systematic review and meta-analysis. *J Dtsch Dermatol Ges* 2018; 16: 1197-1208.
- [3] Lommerts JE, Uitentuis SE, Bekkenk MW, de Rie MA and Wolkerstorfer A. The role of phototherapy in the surgical treatment of vitiligo: a systematic review. *J Eur Acad Dermatol Venereol* 2018; 32: 1427-1435.
- [4] Zheng PJ, Wang CM, Zong ZH and Wang LQ. A new active learning method based on the learning function U of the AK-MCS reliability analysis method. *Eng Struct* 2017; 148: 185-194.
- [5] Mecikalski RM and Carey LD. Lightning characteristics relative to radar, altitude and temperature for a multicell, MCS and supercell over northern Alabama. *Atmos Res* 2017; 191: 128-140.
- [6] Zhang CZ, Zhou L, Huang J, Mei XY, Wu ZW and Shi WM. A preliminary study of growth characteristics of melanocytes co-cultured with keratinocytes in vitro. *J Cell Biochem* 2018; 119: 6173-6180.
- [7] Abdelrahman SA, Samak MA and Shalaby SM. Fluoxetine pretreatment enhances neurogenic, angiogenic and immunomodulatory effects of MSCs on experimentally induced diabetic neuropathy. *Cell Tissue Res* 2018; 374: 83-97.
- [8] Lu Y, Zhu WY, Tan C, Yu GH and Gu JX. Melanocytes are potential immunocompetent cells: evidence from recognition of immunological characteristics of cultured human melanocytes. *Pigment Cell Res* 2002; 15: 454-460.
- [9] Deng B, Wang WH, Deng LL, Yao SX, Ming J and Zeng KF. Comparative RNA-seq analysis of citrus fruit in response to infection with three major postharvest fungi. *Postharvest Biol Tec* 2018; 146: 134-146.
- [10] Zhang JH, Chen SL, Cai J, Hou ZQ, Wang XH, Kachelmeier A and Shi XR. Culture media-based selection of endothelial cells, pericytes, and perivascular-resident macrophage-like melanocytes from the young mouse vestibular system. *Hear Res* 2017; 345: 10-22.
- [11] Haltaufderhyde KD and Oancea E. Genome-wide transcriptome analysis of human epidermal melanocytes. *Genomics* 2014; 104: 482-489.
- [12] Royer-Bertrand B, Torsello M, Rimoldi D, El Zaoui I, Cisarova K, Pescini-Gobert R, Raynaud F, Zografos L, Schalenbourg A, Speiser D, Nicolas M, Vallat L, Klein R, Leyvraz S, Ciriello G, Riggi N, Moulin AP and Rivolta C. Comprehensive genetic landscape of uveal melanoma by whole-genome sequencing. *Am J Hum Genet* 2016; 99: 1190-1198.
- [13] Shukla A and Singh TR. Network-based approach to understand dynamic behaviour of Wnt signaling pathway regulatory elements in colorectal cancer. *Netw Model Anal Health Inform Bioinform* 2018; 7.
- [14] Guo Y, Sun L, Xiao L, Gou R, Fang Y, Liang Y, Wang R, Li N, Liu F, Tang L. Aberrant Wnt/Beta-catenin pathway activation in dialysate-induced peritoneal fibrosis. *Front Pharmacol* 2017; 8: 774.
- [15] Shang H, Hao ZQ, Fu XB, Hua XD, Ma ZH, Ai FL, Feng ZQ, Wang K, Li WX and Li B. Intermedin promotes hepatocellular carcinoma cell proliferation through the classical Wnt signaling pathway. *Oncol Lett* 2018; 15: 5966-5970.
- [16] Li P, Gao Y, Li J, Zhou Y, Yuan J, Guan HW and Yaog P. LncRNA MEG3 repressed malignant melanoma progression via inactivating Wnt signaling pathway. *J Cell Biochem* 2018; 119: 7498-7505.
- [17] Lin YX, Wang FF, Xing QF, Guo F, Wang MZ and Li YJ. The biological effect and mechanism of the Wnt/beta-catenin signaling pathway on malignant melanoma A375 cells. *Exp Ther Med* 2018; 16: 2032-2037.
- [18] Lu W, Zhao Y, Kong Y, Zhang W, Ma W, Li W and Wang K. Geniposide prevents H2O2-induced oxidative damage in melanocytes by activating the PI3K-Akt signalling pathway. *Clin Exp Dermatol* 2018; 43: 667-674.
- [19] Irvine M, Stewart A, Pedersen B, Boyd S, Kefferd R and Rizos H. Oncogenic PI3K/AKT promotes the step-wise evolution of combination BRAF/MEK inhibitor resistance in melanoma. *Oncogenesis* 2018; 7: 72.
- [20] Laugier F, Finet-Benyair A, Andre J, Rachakonda PS, Kumar R, Bensussan A and Dumaz N. RICTOR involvement in the PI3K/AKT pathway regulation in melanocytes and melanoma. *Oncotarget* 2015; 6: 28120-28131.
- [21] Tu PT, Nguyen BC, Tawata S, Yun CY, Kim EG and Maruta H. The serum/PDGF-dependent "melanogenic" role of the minute level of the oncogenic kinase PAK1 in melanoma cells

Screening and analysis of human melanocytes genes

- proven by the highly sensitive kinase assay. *Drug Discov Ther* 2016; 10: 314-322.
- [22] Pazos MC, Sequeira G, Bocchicchio S, May M, Abramovich D, Parborell F, Tesone M and Irusta G. PDGFB as a vascular normalization agent in an ovarian cancer model treated with a gamma-secretase inhibitor. *J Cell Physiol* 2018; 233: 5949-5961.
- [23] Herraiz C, Jimenez-Cervantes C, Sanchez-Laorden B and Garcia-Borrón JC. Functional interplay between secreted ligands and receptors in melanoma. *Semin Cell Dev Biol* 2018; 78: 73-84.
- [24] Jitariu AA, Raica M, Cimpean AM and Suciuc SC. The role of PDGF-B/PDGFR-BETA axis in the normal development and carcinogenesis of the breast. *Crit Rev Oncol Hematol* 2018; 131: 46-52.
- [25] Abolurin OO, Adegbola AJ, Oyelami OA, Adegoke SA and Bolaji OO. Vitamin A deficiency among under-five Nigerian children with diarrhoea. *Afr Health Sci* 2018; 18: 737-742.
- [26] Metzler MA, Raja S, Elliott KH, Friedl RM, Tran NQH, Brugmann SA, Larsen M and Sandell LL. RDH10-mediated retinol metabolism and RAR alpha-mediated retinoic acid signaling are required for submandibular salivary gland initiation (vol 145, dev164822, 2018). *Development* 2018; 145.
- [27] Alonso S, Jones RJ and Ghiaur G. Retinoic acid, CYP26, and drug resistance in the stem cell niche. *Exp Hematol* 2017; 54: 17-25.

Screening and analysis of human melanocytes genes

Table S1. The system of reverse transcription in qPCR verification

	Dosage
Total RNA	3 µg
Anchored-oligo (dT) 18 Primer (50 pmol/µL)	1 µL
Random Hexamer Primer (600 pmol/µL)	2 µL
PCR component	1 µL
Total	13 µL

Table S2. The reaction system of Real-time PCR in qPCR verification

PCR component	Volume (µL)
Mix (RR420)	10
P1 (1 µm/L) 2	2
P2 (1 µm/L) 2	2
DNA 1	1
Water	4.6
ROX	0.4
ROX	20

Table S3. The counts of PAX3+ cells and Melan-A+ cells by MACS in different time points

	P0	P1	P2	P3
Total number of cells	4.0×10^7	1.2×10^7	1.5×10^7	2.5×10^7
Number of cells after sorting	3.7×10^6	1.0×10^6	1.2×10^6	1.9×10^6
Positive rate	9.3%	8.3%	8.0%	7.6%

Table S4. Concentrations and purity of total RNA

Sample	A260/A280	Nano (ng/µL)	Volume (µL)	Total (µg)
P0	1.94	1356	20	27.12
P1	1.96	4756	20	95.12
P2	1.98	1205	25	30.13
P3	1.98	901.2	30	27.00

Table S5. RNA-seq data of 4 samples and mapped results to reference genome

Sample	Total base/bp	n _{Total Reads}	n _{Map reads}	GC Contents %	Q30 ratio
P0	6606474600	44043164	38352714	51.20	89.28
P1	6316460400	42109736	36421365	51.27	88.98
P2	6249647400	41664316	36233760	50.69	89.2
P3	6287661000	41917740	34977997	50.51	84.73

Table S6. The counts of genes at different FPKM levels

FPKM level	P0	P1	P2	P3
0-0.1	40140	43144	43049	43278
0.1-0.5	5303	4584	4613	3838
0.5-5	8437	6166	6172	5803
5-15	4037	3968	4156	3962
15-60	3807	4142	4173	4862
> 60	1930	1650	1491	1911

Screening and analysis of human melanocytes genes

Table S7. The counts of DEGs in different compared groups

Comparable group	DEGs (n)	Up-regulated genes (n)	Down-regulated genes (n)
P1 vs P0	1325	332	993
P2 vs P0	1421	448	973
P3 vs P0	1657	548	1109

Table S8. Top 20 DEGs with increased or decreased FRKM in P1 vs P0 group

Up-regulated				Down-regulated			
Gene name	P0 FPKM	P1 FPKM	<i>p</i> value	Gene name	P0 FPKM	P1 FPKM	<i>p</i> value
MIR3661	0	1252.03	0.0105	MT-TL1	88107.9	0	0.0259
MIR635	0	1090.67	0.0099	MIR4668	21627.5	0	0.03875
AREGB	30.5751	554.196	0.0032	MT-RNR2	20432	1727.95	0.03915
AREG	30.0061	545.351	0.00255	RP5-1052M9.1	11495.3	0	0.0363
IFI6	26.4341	534.486	0.00225	SNORD99	9209.12	0	0.0291
ASS1	20.6652	350.763	0.00635	KRT1	8548.88	1.56992	0.0017
LAMC2	16.919	336.053	0.01025	KRTDAP	8156.54	25.894	0.00125
MMP1	4.82E+01	357.895	0.0465	SPRR1B	6120.74	173.658	0.00825
AC022596.6	7.93199	308.795	0.0065	DMKN	5343.74	185.308	0.012
ITGB1	45.202	334.704	0.04665	KRT10	5119.68	19.7715	0.03375
KRT7	22.4924	299.597	0.01135	NFKBIA	3220.3	105.281	0.0259
TRIB3	41.3588	305.15	0.0293	SPRR1A	3091.25	25.1399	0.00115
COL6A3	25.0408	280.113	0.0486	GADD45B	3077.45	31.7094	0.00715
ANXA3	25.9657	268.929	0.01245	SBSN	2944.44	24.5776	0.00485
PSAT1	28.2478	236.191	0.0206	ZFP36	2947.22	59.7202	0.0238
LDHB	17.2798	209.914	0.0062	PI3	2579.2	19.784	0.00055
F3	32.8758	209.526	0.0359	MT-ND6	2893.65	368.936	0.03405
TP63	25.3428	191.397	0.03225	CALML5	2106.32	3.51726	0.01165
TM7SF3	7.66283	169.628	0.0057	CCL20	1762.07	3.9687	0.0035
DKK3	27.8796	186.557	0.0398	LY6D	1733.67	64.5883	0.0039

Table S9. Top 20 DEGs with increased or decreased FRKM in P2 vs P0 group

Up-regulated				Down-regulated			
Gene name	P0 FPKM	P2 FPKM	<i>p</i> value	Gene name	P0 FPKM	P2 FPKM	<i>p</i> value
IL6	129.565	1277.95	0.03475	MT-TL1	87181.2	0	0.02455
DCN	104.118	1164.89	0.04995	MIR4668	21400	0	0.0312
IFI6	26.1561	601.945	0.0059	MT-RNR2	20217.1	1452.26	0.04185
RP1-206D15.5	0	445.256	0.01105	RP5-1052M9.1	11374.4	0	0.03855
TYRP1	25.3798	421.31	0.017	KRT1	8458.96	1.2671	0.0061
ANPEP	22.253	409.1	0.01995	KRTDAP	8070.75	5.1272	0.01455
IL11	2.97998	347.727	0.00265	SPRR1B	6056.36	92.3134	0.00565
GREM1	3.25656	340.299	0.0006	DMKN	5287.53	38.8153	0.00305
LDHB	17.098	344.852	0.00495	SPRR1A	3058.74	10.6306	0.0024
WNT5A	4.62385	321.32	0.00285	GADD45B	3045.08	42.197	0.01865
COL3A1	17.7551	323.706	0.02475	SBSN	2913.47	16.0612	0.00575
MME	5.54242	272.844	0.00645	ZFP36	2916.22	49.6625	0.03205
CTSK	18.3348	279.263	0.0104	PI3	2552.07	17.5064	0.0021
IL1B	27.6103	285.348	0.0213	LGALS7B	2098.51	144.262	0.01435
FKBP10	15.6804	240.29	0.0133	CCL20	1743.54	25.327	0.0014

Screening and analysis of human melanocytes genes

CXCL5	6.06663	204.903	0.00255	LY6D	1715.44	25.971	0.0013
PRRX1	10.7855	197.116	0.0168	FXYD3	1494.33	177.009	0.0355
HTRA1	20.3769	206.318	0.02085	LYPD3	1198.97	15.2081	0.00345
CALU	16.759	190.229	0.01765	CRABP2	1149.57	60.1063	0.0118
AKR1B1	21.6271	194.147	0.02715	RP11-544M22.13	0	4.51073	0.05005

Table S10. Top 20 DEGs with increased or decreased FRKM in P3 vs P0 group

Up-regulated				Down-regulated			
Gene name	P0 FPKM	P3 FPKM	p value	Gene name	P0 FPKM	P3 FPKM	p value
MMP1	48.006	2523.11	0.0474	MT-TL1	87810.3	0	0.0311
IFI6	26.3449	722.689	0.0062	MIR4668	21554.4	0	0.00755
ASS1	20.5954	682.813	0.01015	MT-RNR2	20363	1055.69	0.02515
ANPEP	22.4136	642.685	0.0268	RP5-1052M9.1	11456.5	0	0.02705
CTSK	18.4672	613.358	0.00685	SPRR1B	6100.07	7.59925	0.0127
MME	5.58244	500.661	0.00585	DMKN	5325.69	13.2127	0.0005
LTBP1	7.6188	400.804	0.00885	GADD45B	3067.06	93.3176	0.04895
LDHB	17.2214	404.645	0.00825	SBSN	2934.49	6.94635	0.0055
AL353629.1	0	345.276	0.0286	S100A14	2647.37	61.146	0.0189
TYRP1	25.5629	361.002	0.03165	LGALS7B	2113.66	31.5455	0.005
FKBP10	15.7935	318.691	0.012	CCL20	1756.12	7.58453	0.00315
ASPH	16.3409	310.936	0.025	LY6D	1727.82	1.66881	0.02635
COL3A1	17.8832	308.901	0.03445	S100A9	1634.15	76.3584	0.01255
THY1	10.0166	292.49	0.0115	FXYD3	1505.12	35.9182	0.00525
TWIST2	12.3081	279.42	0.0126	S100A8	1395	30.3976	0.00565
NT5E	3.25659	260.153	0.00145	LYPD3	1207.62	7.78693	0.0039
HTRA1	20.524	274.963	0.0215	CRABP2	1157.87	64.6802	0.0195
CRTAP	21.3571	257.929	0.04975	RHCG	1092.41	0.392596	0.0088
FAM20C	8.09314	234.63	0.00795	AQP3	1037.16	1.31305	0.0052
SCD	3.0477	218.009	0.00425	TRIM29	1047.29	13.8448	0.00645

Table S11. GO analysis of DEGs in different compared groups

Comparable group	BP (n)	CC (n)	MF (n)
P1 vs P0	127	28	34
P2 vs P0	101	26	39
P3 vs P0	140	28	54

Table S12. Top 10 pathways with the most DEGs in different compared groups

	Term	Count
P1 vs P0	hsa04060:Cytokine-cytokine receptor interaction	18
	hsa04010:MAPK signaling pathway	17
	hsa05166:HTLV-I infection	16
	hsa04062:Chemokine signaling pathway	13
	hsa05169:Epstein-Barr virus infection	11
	hsa04514:Cell adhesion molecules (CAMs)	10
	hsa04630:Jak-STAT signaling pathway	10
	hsa04668:TNF signaling pathway	9
	hsa04650:Natural killer cell mediated cytotoxicity	9
	hsa05164:Influenza A	9

Screening and analysis of human melanocytes genes

P2 vs P0	hsa04060:Cytokine-cytokine receptor interaction	13
	hsa00590:Arachidonic acid metabolism	9
	hsa04640:Hematopoietic cell lineage	9
	hsa05162:Measles	9
	hsa04630:Jak-STAT signaling pathway	9
	hsa04514:Cell adhesion molecules (CAMs)	8
	hsa05146:Amoebiasis	7
	hsa05144:Malaria	6
	hsa05150:Staphylococcus aureus infection	6
	hsa00982:Drug metabolism - cytochrome P450	6
P3 vs P0	hsa04060:Cytokine-cytokine receptor interaction	15
	hsa04062:Chemokine signaling pathway	14
	hsa04650:Natural killer cell mediated cytotoxicity	12
	hsa04014:Ras signaling pathway	12
	hsa00590:Arachidonic acid metabolism	9
	hsa04670:Leukocyte transendothelial migration	9
	hsa04360:Axon guidance	9
	hsa04514:Cell adhesion molecules (CAMs)	9
	hsa04660:T cell receptor signaling pathway	8
	hsa04270:Vascular smooth muscle contraction	8

Table S13. Top 10 pathways including most DEGs with increased or decreased expression

	Term	Count
Continuously up-regulated	hsa01100:Metabolic pathways	174
	hsa05200:Pathways in cancer	64
	hsa04151:PI3K-Akt signaling pathway	52
	hsa04510:Focal adhesion	44
	hsa01130:Biosynthesis of antibiotics	38
	hsa04810:Regulation of actin cytoskeleton	35
	hsa04142:Lysosome	34
	hsa05205:Proteoglycans in cancer	33
	hsa04015:Rap1 signaling pathway	33
	hsa04141:Protein processing in endoplasmic reticulum	30
Continuously down-regulated	hsa01100:Metabolic pathways	91
	hsa04010:MAPK signaling pathway	23
	hsa05010:Alzheimer's disease	22
	hsa00190:Oxidative phosphorylation	20
	hsa04530:Tight junction	17
	hsa04932:Non-alcoholic fatty liver disease (NAFLD)	17
	hsa05012:Parkinson's disease	15
	hsa04360:Axon guidance	14
	hsa04670:Leukocyte transendothelial migration	13
	hsa04750:Inflammatory mediator regulation of TRP channels	12

Screening and analysis of human melanocytes genes

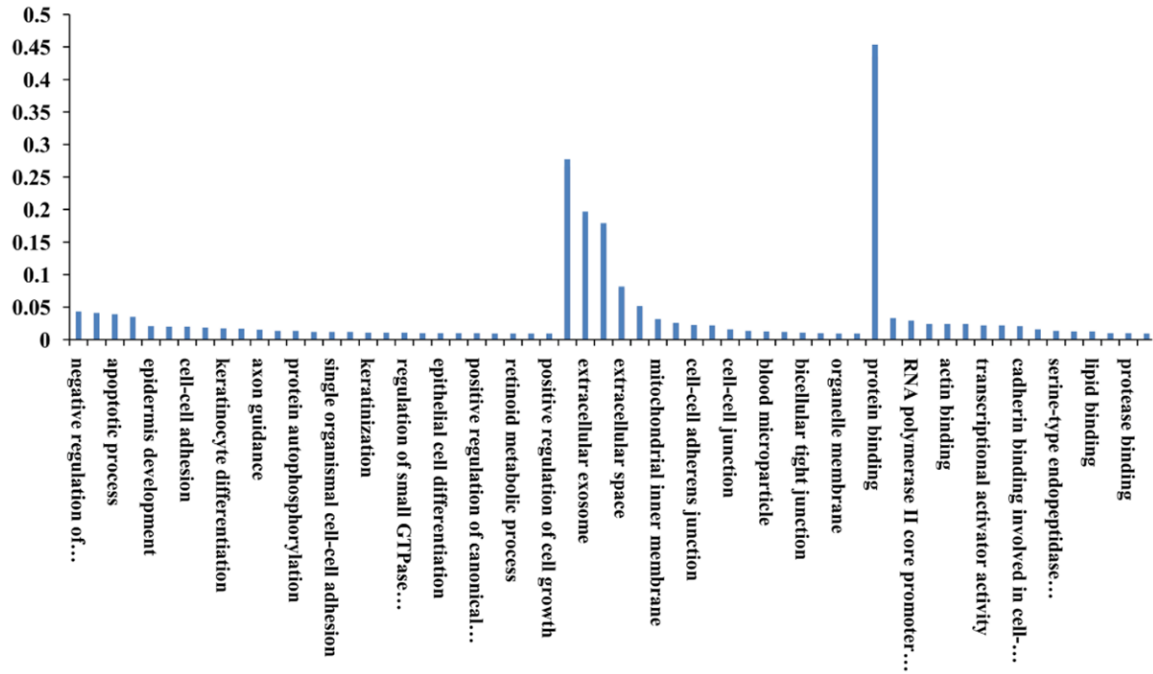


Figure S1. GO analysis of DEGs with continuously decreased expression.

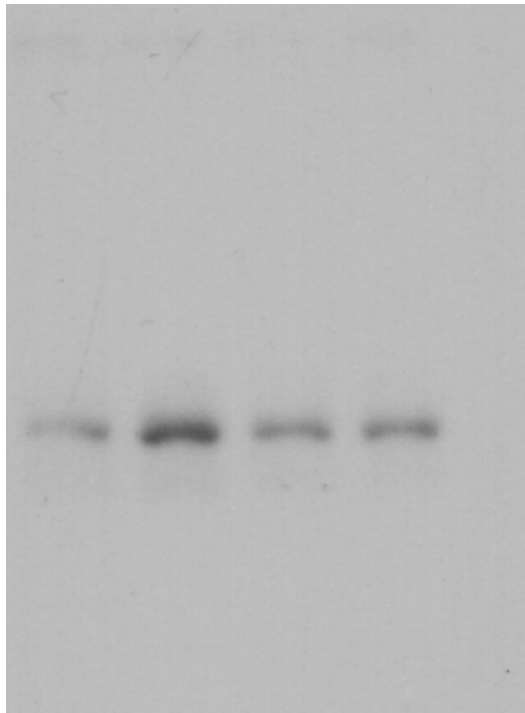


Figure S2. Original Western blot images of AKT3 in Figure 7.

Screening and analysis of human melanocytes genes

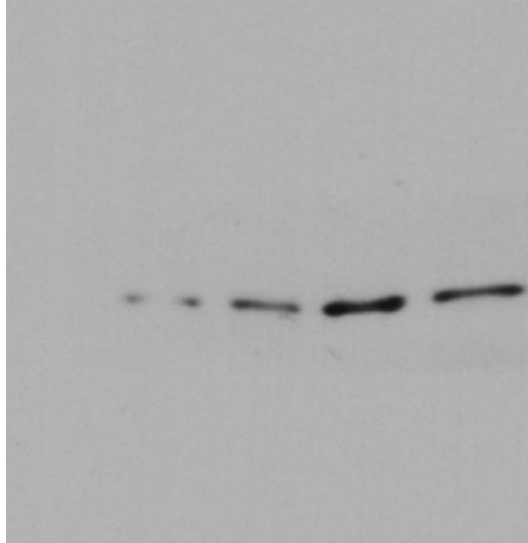


Figure S3. Original Western blot images of ITGA7 in **Figure 7**.

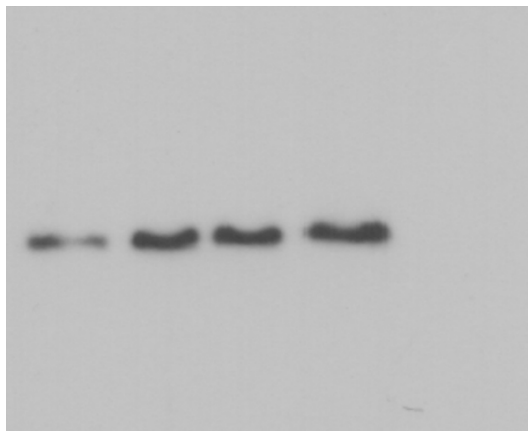


Figure S4. Original Western blot images of PIK3R2 in **Figure 7**.

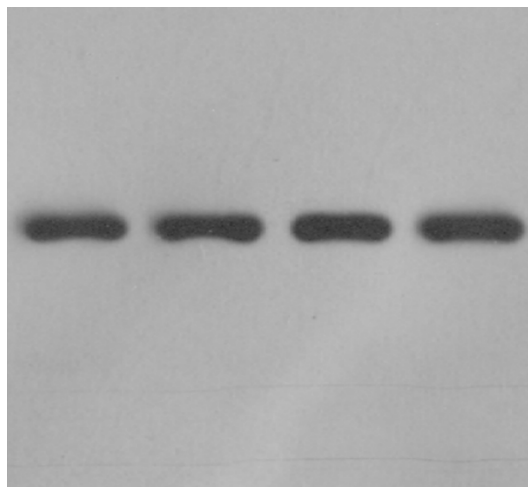


Figure S5. Original Western blot images of GAPDH in **Figure 7**.

Screening and analysis of human melanocytes genes

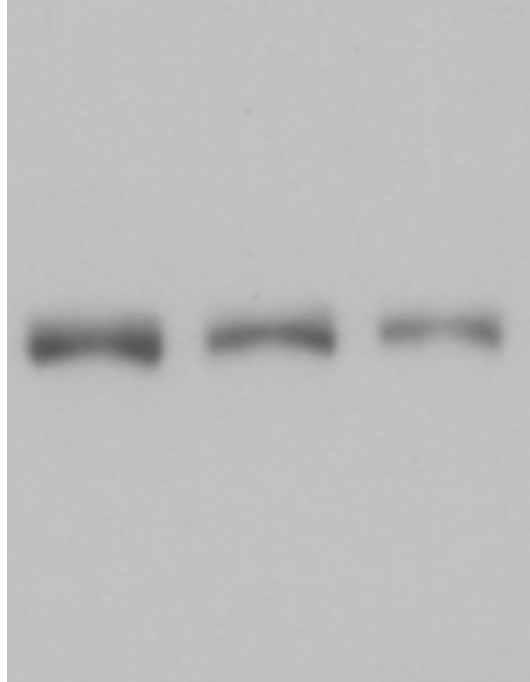


Figure S6. Original Western blot images of PDGFB in **Figure 8.**

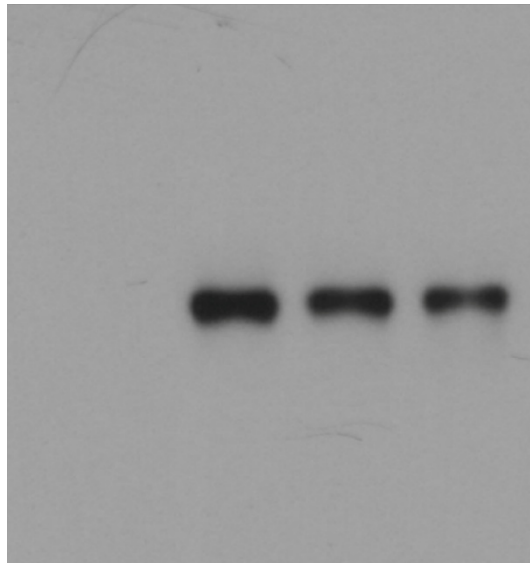


Figure S7. Original Western blot images of RDH10 in **Figure 8.**

Screening and analysis of human melanocytes genes

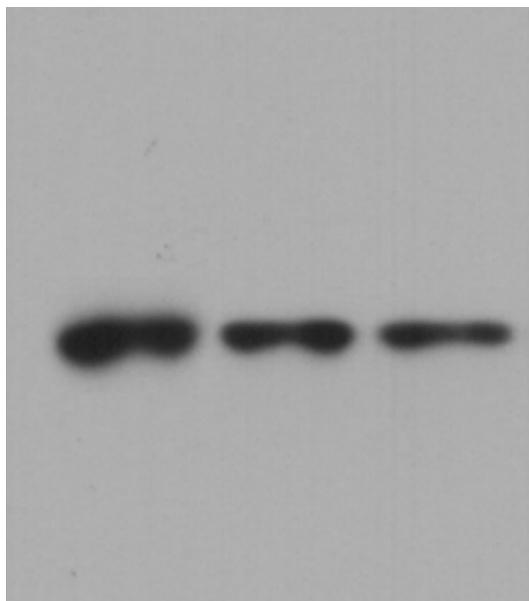


Figure S8. Original Western blot images of DHR3 in **Figure 8**.

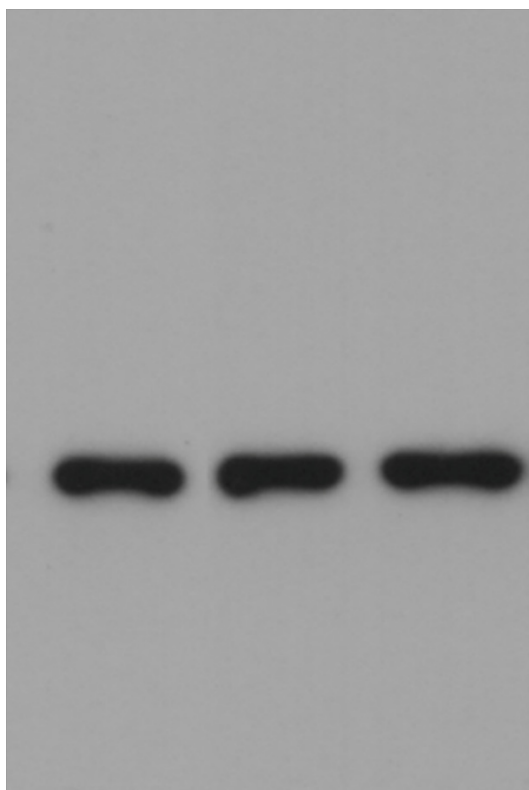


Figure S9. Original Western blot images of GAPDH in **Figure 8**.